

# Journal of Intelligent Material Systems and Structures

<http://jim.sagepub.com/>

---

## **Application of single unit impact dampers to harvest energy and suppress vibrations**

Aref Afsharfard and Anooshiravan Farshidianfar

*Journal of Intelligent Material Systems and Structures* 2014 25: 1850 originally published online 14 May 2014

DOI: 10.1177/1045389X14535012

The online version of this article can be found at:

<http://jim.sagepub.com/content/25/14/1850>

---

Published by:



<http://www.sagepublications.com>

**Additional services and information for *Journal of Intelligent Material Systems and Structures* can be found at:**

**Email Alerts:** <http://jim.sagepub.com/cgi/alerts>

**Subscriptions:** <http://jim.sagepub.com/subscriptions>

**Reprints:** <http://www.sagepub.com/journalsReprints.nav>

**Permissions:** <http://www.sagepub.com/journalsPermissions.nav>


**Citations:** <http://jim.sagepub.com/content/25/14/1850.refs.html>

>> [Version of Record](#) - Sep 3, 2014

[OnlineFirst Version of Record](#) - May 14, 2014

[What is This?](#)

# Application of single unit impact dampers to harvest energy and suppress vibrations

Journal of Intelligent Material Systems and Structures  
2014, Vol. 25(14) 1850–1860  
© The Author(s) 2014  
Reprints and permissions:  
sagepub.co.uk/journalsPermissions.nav  
DOI: 10.1177/1045389X14535012  
jim.sagepub.com  


Aref Afsharfard and Anooshiravan Farshidianfar

## Abstract

In this study, ongoing investigations to apply piezoelectric materials as an energy harvester are extended. In doing so, effectiveness of single unit impact dampers is increased using piezoelectric materials. For this reason, barriers of the impact damper are replaced with cantilever beams, which are equipped with the piezoelectric patches. For convenience, this kind of impact dampers is named as “piezo-impact dampers.” The piezo-impact damper is not only a vibration suppressor but also it is an energy harvester. An analytical approach is presented to formulate the voltage and power generation in the barriers of the piezo-impact dampers. Variation in output voltage is studied with changing the main parameters of the piezo-impact damper. Furthermore, damping inclination, which presents the ability of vibration suppressing in impact dampers, is calculated with varying the main parameters of the impact damper. Regarding calculated output voltage and damping inclination in the piezo-impact dampers, two “energy-based” and “vibratory-based” design methods are presented. Finally, using several user-oriented charts, the discussed design methods are combined to provide a powerful piezo-impact damper.

## Keywords

Energy harvesting, piezoelectric materials, impact damper, damping inclination

## Introduction

The piezoelectric materials can widely be used in structures to improve their application. For example, the aerospace structures may be equipped with the piezoelectric devices to increase the damping and subsequently reduce the amplitude of undesired vibrations. Agneni et al. (2003) presented a procedure to analyze effectiveness of the shunted piezoelectric devices in increasing passive damping of elastic and aeroelastic systems. They showed that these devices are able to reduce the gust response amplitude of glider wings, whenever it is in the neighborhood of the flutter instability. They proposed an optimal strategy to evaluate the electrical load for tuning the piezo devices, as function of the flight speed. Agneni and Coppotelli (2004) showed the natural frequencies and damping ratios of a structure, which is equipped with shunted piezo devices, depend on the electrical load. They presented an approach, which provide a method to predict not only the natural frequency of the structure but also the maximum damping ratio introduced by the piezo devices.

Nowadays, the field of energy harvesting has been extensively considered by researchers. The reason for

this interest lies in the fact that hundreds of millions of people need to have access to clean and modern energies. The ability of piezoelectric materials to convert mechanical energy into electrical energy made them interesting devices to use as energy harvesters (Annanddas and Radhika, 2013; Green et al., 2013; Tang et al., 2010).

Previous studies indicate extensive applications for the piezoelectric energy harvesters as a prospective alternative for the batteries. Erturk et al. (2010) used a piezoaeroelastic airfoil to harvest energy at its flutter boundary. They studied the effect of piezoelectric power generation on the linear flutter speed. Mehmood et al. (2013) studied the concept of harvesting energy using a circular cylinder undergoing vortex-induced vibrations. They showed that increasing the load resistance leads to increase in output voltage. Abdelkefi

---

Department of Mechanical Engineering, Ferdowsi University of Mashhad, Mashhad, Iran

### Corresponding author:

Aref Afsharfard, Department of Mechanical Engineering, Ferdowsi University of Mashhad, Mashhad, Iran.  
Email: Aref.Afsharfard@gmail.com

et al. (2013b) attached a piezoelectric transducer to galloping oscillator for harvesting energy. They studied the effects of changing load resistance, cross-sectional geometry, and stream velocity on power generation. Pozzi and Zhu (2012) investigated a knee-joint wearable energy harvester. They found that the speed at which plectra and bimorph come into contact strongly influences the energy production. Moss et al. (2013) experimentally studied a vibro-impact energy harvester. They also explored the damage to the barriers caused by the impacting process. Jacquelin et al. (2011) presented an impact energy harvester system. De Jong et al. (2013) simulated a piezoelectrically augmented helicopter lag damper to harvest electrical energy. They optimized the design parameters of the system to improve its application. Kim et al. (2013) presented a rotational energy harvester using wind-induced vibration of inclined stay cables. They showed that this device can generate sufficient electricity to power a wireless sensor node placed on a cable. Abdelkefi et al. (2013b) used the transverse galloping of bluff bodies for energy harvesting. They concluded that the maximum levels of harvested power can be accompanied with minimum transverse displacement amplitude of the system. Abdelkefi et al. (2013b, 2014) showed that vibration amplitude suppression, in the galloping oscillator energy harvesters, can be accompanied by power enhancement. They explained this result by the resistive shunt damping effect. De Marqui and Erturk (2013) analyzed airfoil-based aeroelastic energy harvesters. They studied the effect of system parameters on the harvested electrical power.

Although application of energy harvester has been extensively investigated, there are still several shortcomings in this area of research that should be noted. Usually, the energy harvesters are studied as a main system, which only generate energy. In other words, usually, the energy harvesters were not studied as a subsystem in a practical system, which does its main duties. Note that the main duties of the practical system may not be energy harvesting. Therefore, two following questions may be posed:

- Can the energy harvesters, like piezoelectric devices, be employed in a practical system, which is not originally designed only for energy harvesting?
- What is the effect of using the energy harvesters on the main application of the practical systems?

In this study, application of a passive control device equipped with an energy harvester is studied. Passive control devices, including base isolation, friction dampers, viscous fluid dampers, impact dampers, tuned mass dampers, and tuned liquid dampers, are accepted means for mitigating the effects of dynamic loadings (Ibrahim, 2009; Soong and Spencer, 2002; Zinjade and

Mallik, 2007). An inner mass single unit impact damper, or simply "impact damper," is a small loose mass, which can move freely in an enclosure connected to a main vibratory mass. When the vibration amplitude of the main mass exceeds than the gap size, the impact mass collides with main mass barriers. Consequently, the kinetic energy of the main mass is absorbed and converted into heat and sound through inelastic collisions. These systems can be extensively applied to attenuate the undesirable vibration of robot arms, turbine blades, and so on (Dimentberg and Iourtchenko, 2004; Zhang and Angeles, 2005). In the past few years, the behavior of impact dampers has been investigated experimentally, analytically, and numerically (Afsharfard and Farshidianfar, 2012a, 2012b; Cheng and Wang, 2003; Cheng and Xu, 2006). Bapat and Sankar (1985) showed that the coefficient of restitution has a great effect on the performance of impact dampers. They demonstrated that in the case of single unit impact dampers, optimized parameters at resonance are not necessarily optimal at other frequencies. Popplewell and Liao (1991) introduced an accurate approximation to determine the optimum clearance of a rigid damper. Son et al. (2010) proposed active momentum exchange impact dampers to suppress the first large peak value of the acceleration response due to a shock load. They showed that increasing the coefficient of restitution may lead to an increase in the reliability of the vibratory systems. Ema and Marui (1994) investigated the characteristics of an impact damper in free damped vibration. They indicated that the damping capability of the vibratory system could be significantly improved using a proper impact damper.

The main target of this study is to analyze the vibratory behavior of a system, which is equipped with an impact damper. As mentioned before, impact dampers convert the kinetic energy into useless energy, such as heat and sound. To improve the application of the impact dampers, each barrier of these systems is equipped with a piezoelectric device, which converts undesired energy into a useful form of energy. Therefore, instead of wasting the undesired mechanical energy, it can be gathered and saved. In this study, this kind of impact dampers is simply named as piezo-impact damper. Unlike the conventional impact damper, the piezo-impact damper is not only a vibration suppressor but also an energy harvester.

The main and secondary applications of the piezo-impact damper are vibration suppressing and energy harvesting. The effect of using the energy harvester on the main application of the piezo-impact damper is investigated. To improve application of the piezo-impact damper, the initial design of this system is divided into "energy-based" and "vibratory-based" designs. As both the design methods are initially considered, the piezo-impact damper can effectively suppress vibrations and harvest energy. In doing so, several

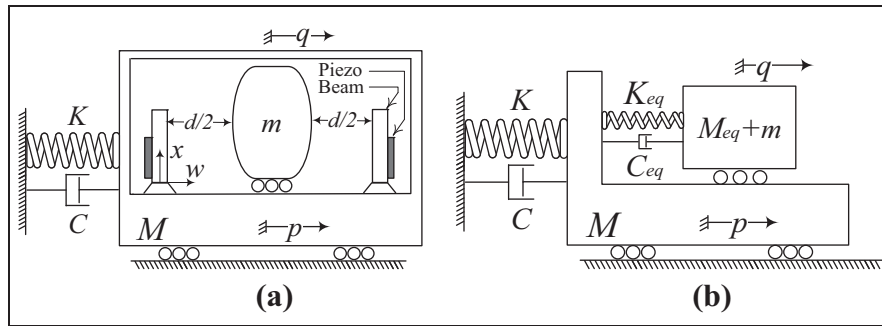


**Figure 1.** (a) Schematic diagram of a vibratory system with an impact damper and (b) schematic while the impact mass collides the main mass.

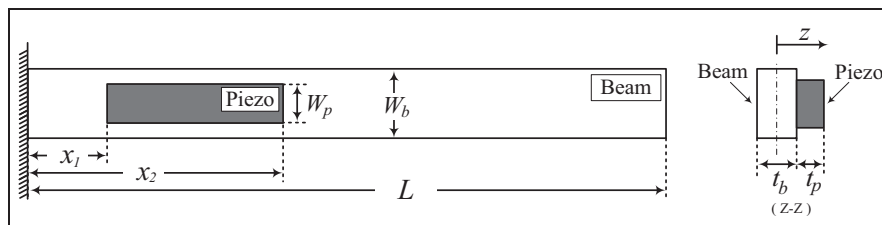


**Figure 2.** Metallic beam with piezoelectric element.

user-oriented charts are presented to help the designer to combine the discussed design methods.

**Piezo-impact damper systems**

*Modeling a vibratory system with an impact damper (piezo-impact damper)*

Schematic model of a vibratory system equipped with an impact damper with impact mass  $m$ , gap size  $d$ , linear stiffness  $K$ , main mass  $M$ , and viscous damping  $C$  is illustrated in Figure 1(a). As shown in Figure 2(b), when  $|p - q| < d/2$ , the impact mass moves freely at a constant speed without causing any collision (free flight of the impact mass). Therefore, differential equations of motion between impacts can be given by

$$\begin{cases} M\ddot{p} + C\dot{p} + Kp = 0 & (1) \\ m\ddot{q} = 0 & (2) \end{cases}$$

In this study, the barriers of the impact damper are the clamped-free beams, which are equipped with the piezoelectric patches. These impact dampers are simply named as “piezo-impact dampers.” When  $|p - q| \geq d/2$ , the impact mass collides with the main mass. Vibratory behavior of the impact damper system can be described using a 2-degree-of-freedom (DOF) system, which is shown in Figure 2(b). To define the energy loss during each contact, the viscous damper  $C_{eq}$  is added in parallel with the springs, which present the contact elastic stiffness. Dynamic behavior of the 2-DOF system can be presented using the following equations

$$\begin{cases} M\ddot{p} + C\dot{p} + Kp - C_{eq}(\dot{q} - \dot{p}) - K_{eq}(q - p) = 0; & p(0) = p_0, \dot{p}(0) = \dot{p}_0 & (3) \\ (M_{eq} + m)\ddot{q} + C_{eq}(\dot{q} - \dot{p}) + K_{eq}(q - p) = 0; & q(0) = q_0, \dot{q}(0) = \dot{q}_0 & (4) \end{cases}$$

where  $K_{eq}$  and  $C_{eq}$  are the equivalent contact stiffness and the equivalent contact damping coefficient, respectively.

In the case of the impact dampers, the equivalent contact stiffness and damping are usually much bigger than the main mass stiffness and damping. Therefore, for simplicity, the stiffness and damping of the main mass are considered negligible. Consequently, equations (3) and (4) can be rewritten as follows

$$\begin{cases} M(\ddot{q} - \ddot{r}) - C_{eq}\dot{r} - K_{eq}r = 0; & r(0) = r_0, \dot{r}(0) = \dot{r}_0 & (5) \\ m_{eq}\ddot{q} + C_{eq}\dot{r} + K_{eq}r = 0; & q(0) = q_0, \dot{q}(0) = \dot{q}_0 & (6) \end{cases}$$

where  $r$  is the relative displacement of the colliding masses ( $r = q - p$ ) and  $m_{eq}$  is the equivalent mass of the impact mass during the contact ( $m_{eq} = M_{eq} + m$ ). Regarding equations (5) and (6), the relative displacement of the masses during the contact is calculated as follows

$$r(t) = \frac{-2m_{eq}M\dot{r}_0 \sin\left(\frac{\sqrt{4K_{eq}m_{eq}M(m_{eq} + M) - C_{eq}^2(m_{eq} + M)^2}}{2m_{eq}M}t\right)}{\sqrt{4K_{eq}m_{eq}M(m_{eq} + M) - C_{eq}^2(m_{eq} + M)^2}^{3/2}} \exp\left(-C_{eq}\frac{m_{eq} + M}{2m_{eq}M}t\right) \quad (7)$$

Because the equivalent contact stiffness ( $K_{eq}$ ) is often a high value, the maximum relative displacement of the collided masses can accurately be given by

$$r_{max} = -\frac{2m_{eq}M\dot{r}_0}{\sqrt{4K_{eq}m_{eq}M(m_{eq} + M) - C_{eq}^2(m_{eq} + M)^{3/2}}} \exp\left(\frac{-\pi C_{eq}\sqrt{m_{eq} + M}}{\sqrt{4K_{eq}m_{eq}M - C_{eq}^2(m_{eq} + M)^{1/2}}}\right) \quad (8)$$

The maximum value of the relative displacement of the masses, which is shown in the above equation, is equal to the tip deflection of the cantilever beam (the barrier) that is shown in Figure 2(a).

**Mathematical model of the piezo-impact damper barriers**

Top view and cross-sectional view of a clamped-free beam equipped with a piezoelectric patch is shown in Figure 2. The thickness of the beam is  $t_b$  and its length is equal to  $L$ . The piezoelectric film thickness is  $t_p$  and its length is  $x_2 - x_1$ . The piezoelectric patch is attached to the beam at distance  $x_1$ , which is measured from the clamped edge of the beam.

In this study, it is assumed that there is no axial deformation for the beam. Furthermore, it is considered that the beam cross section is uniform and the Euler-Bernoulli beam assumptions are satisfied. The transverse displacement of the cantilever beam and the governing equation of the strain-voltage relation are as follows (Abdelkefi et al., 2013a; Erturk and Inman, 2008)

$$m(x)\frac{\partial^2 w(x,t)}{\partial t^2} + c_a\frac{\partial w(x,t)}{\partial t} + YI(x)\frac{\partial^4 w(x,t)}{\partial x^4} + v_p V(t)\left\{\frac{d\delta(x-x_1)}{dx} - \frac{d\delta(x-x_2)}{dx}\right\} = F_c\delta(x-L) \quad (9)$$

$$e_{31}W_p\frac{(t_b + t_p)}{2}\int_{x_1}^{x_2}\frac{\partial^3 w(x,t)}{\partial x^2\partial t}dx + \frac{\epsilon_{33}W_p(x_2 - x_1)}{t_p}\frac{dV(t)}{dt} + \frac{1}{R}V(t) = 0 \quad (10)$$

In the above relations,  $w$  is the relative lateral vibration of the cantilever beam;  $m$  is the mass per unit length;  $Y$  is the Young's modulus;  $c_a$  is the viscous damping coefficient;  $I$  is the moment of inertia;  $v_p$  is the piezoelectric coupling term;  $F_c$  is the contact force, which can be obtained using the linear momentum concept;  $\delta$  is the Dirac delta function;  $e_{31} = Y_p d_{31}$  is the piezoelectric stress coefficient;  $W_p$  is the piezoelectric patch width; and  $\epsilon_{33}$  is the permittivity component at

constant strain. The variables  $m(x)$  and  $YI(x)$  are defined using the following relations

$$m(x) = \rho_b t_b W_b + \rho_p t_p W_p \{H(x - x_1) - H(x - x_2)\} \quad (11)$$

$$YI(x) = YI_b + YI_p \{H(x - x_1) - H(x - x_2)\} \quad (12)$$

where the superscripts  $b$  and  $p$  represent the beam and the piezoelectric properties, respectively;  $H(x)$  is the Heaviside step function;  $\rho$  is the mass density;  $W$  is the width; and  $I$  is the moment of inertia. Note that the effect of the presence of the piezoelectric patch on the elastic behavior of the beam is considered in  $m$  and  $Y$ , which are variables along the beam length. In equation (12),  $YI_b$  and  $YI_p$  are as follows

$$YI_b = \frac{Y_b W_b t_b^3}{12} \quad (13)$$

$$YI_p = \frac{Y_p W_p t_p}{12} \{t_p^2 + 3(t_p + t_b - 2z_n)^2\} \quad (14)$$

where  $z$  is the distance (in  $z$  direction) measured from the geometric center of the beam and  $z_n$  is the distance to the neutral surface. For the portions where piezoelectric is bonded ( $x_1 < x < x_2$ ),  $z_n$  is given by the following relation

$$z_n = \frac{Y_p t_p}{Y_b t_b + Y_p t_p} (t_b + t_p) \quad (15)$$

Equations (9) and (10) can accurately be studied using the method of Ritz in conjunction with the principle of virtual displacements (Ba'zant and Cedolin, 2010; Simites and Hodges, 2006). Truncated series involving a complete set of basis function, which can be used to show the transverse displacements, is given by

$$w(x,t) = \sum_{i=0}^N \lambda_i(t) \cdot \phi_i(x) \quad (16)$$

where  $\lambda_i$  is the time-dependent response and  $\phi_i$  is the uniform cantilever beam free vibration mode shape. The uniform cantilever beam mode shapes can be written as follows (Erturk and Inman, 2008; Palm, 2007; Thomson, 1993)

$$\phi_i(x) = C_i \{ \cosh(\beta_i x) - \cos(\beta_i x) - \kappa_i (\sinh(\beta_i x) - \sin(\beta_i x)) \} \quad (17)$$

In the above equation, the coefficient  $\kappa_i$  is defined as follows

$$\kappa_i = \frac{\sinh(\beta_i L) - \sin(\beta_i L)}{\cosh(\beta_i L) + \cos(\beta_i L)} \quad (18)$$

In the cantilever beams,  $\cos(\beta_i L) \cdot \cosh(\beta_i L) + 1 = 0$ , so that  $\beta_1 L = 1.8751$ ,  $\kappa_1 = 0.7341$ , and  $C_1 = 0.5$ . The calculated mode shapes can be



normalized as shown in the following relation such that, for all  $i$  and  $j$

$$\int_0^L \phi_i \phi_j dx = \begin{cases} \eta_i, & \text{if } i = j \\ 0, & \text{if } i \neq j \end{cases} \quad (19)$$

In the above relation, when  $i = 1$ , the above integral is equal to  $\eta_1 = 0.25L$ . Substituting the truncated series into equations (9)–(10) results in a system of linear coupled ordinary differential equations, which can be given as follows (Abdelkefi et al., 2013a; Erturk and Inman, 2008)

$$M_{eq} \ddot{\lambda}(t) + C_{eq} \dot{\lambda}(t) + K_{eq} \lambda(t) = F_{eq}(t) - \chi V(t) \quad (20)$$

$$C_p \dot{V}(t) + V(t)/R - \chi \dot{\lambda}(t) = 0 \quad (21)$$

where  $\chi = (\phi'(x_2) - \phi'(x_1))v_p$  is the piezoelectric coupling term,  $C_p = \epsilon_{33} W_p (x_2 - x_1) / t_p$  is the capacitance of the harvester and the equivalent damping ( $C_{eq}$ ) is equal to  $C_{eq} = 2\xi(K_{eq} M_{eq})^{1/2}$ . Furthermore, the equivalent mass ( $M_{eq}$ ), stiffness ( $K_{eq}$ ), and contact force ( $F_{eq}$ ) can be calculated using the following relations

$$M_{eq} = \rho_b t_b W_b \eta_1 + \rho_p t_p W_p \int_{x_1}^{x_2} \phi_1^2(x) dx \quad (22)$$

$$K_{eq} = EI_b \eta_1 \beta_1^4 + EI_p \beta_1^4 \int_{x_1}^{x_2} \phi_1^2(x) dx \quad (23)$$

$$F_{eq}(t) = \int_0^L F_c \phi_1(L) dx \quad (24)$$

In the above equations, because the piezoelectric layer does not cover the whole cantilever beam, the vibratory properties ( $M_{eq}$ ,  $K_{eq}$ , and  $C_{eq}$ ) vary along the beam. It should be noted that to increase modeling accuracy, the mode shape should be divided into different regions (Abdelkefi et al., 2013c; Zhao et al., 2013). In the case of piezo-impact dampers, the contacts between masses cause rapid deflection in the cantilever beam (barriers) and may lead to destroy the piezoelectric device. To keep the piezo-device from destroying, small piezoelectric patches should be used in the barriers. Therefore, in the case of the piezo-impact dampers, the piezoelectric coupling term ( $\chi$ ) is small. Furthermore, the contact force ( $F_c$ ) is a high force applied over a short time period. Consequently, it can be concluded that in piezo-impact dampers, the contact force is much bigger than the piezoelectric coupling term, so that the second term in the right-hand side of equation (20) can be neglected. Then the output voltage from the piezoelectric device can be approximated using the relation between voltage and strain of the beam. In doing so, assume that the materials are linear,

elastic, and isotropic with an average stress, which is applied along the 1–1 direction. Therefore, the output voltage from the piezoelectric device can be given by (Priya and Inman, 2008)

$$V(x) = g_{31} \epsilon_x Y_p (x_2 - x_1) \quad (25)$$

where  $g_{31}$  is the piezoelectric voltage constant. The strain on surface of beam at a distance  $y$  from the neutral axis can be represented as follows (Dadfarnia et al., 2004; Priya and Inman, 2008; Sadd, 2009; Ugural and Fenster, 2011)

$$\epsilon_x = \frac{\partial u_x}{\partial x} = -y \frac{\partial^2 w(x, t)}{\partial x^2} \quad (26)$$

where  $u_x$  is the beam displacement field in  $x$  directions. The relation between the beam curvature and the tip deflection is  $\partial^2 w / \partial x^2 = \beta_i^2 \{ \cosh(\beta_i x) + \cos(\beta_i x) - \kappa_1 (\sinh(\beta_i x) + \sin(\beta_i x)) \} w(L)$ . Therefore, using equations (25) and (26), the output voltage from piezoelectric device is as follows

$$V(x) = \beta_1^2 g_{31} L_p E_p (z_n - z) \{ \cosh(\beta_1 x) + \cos(\beta_1 x) - \kappa_1 (\sinh(\beta_1 x) + \sin(\beta_1 x)) \} w(L) \quad (27)$$

Using equations (8) and (27), a relation for the maximum output voltage from piezoelectric patch, which is connected to the beam, can be estimated using the maximum relative displacement of the impact mass and the main mass during the contact ( $|p - q| \geq d/2$ )

$$V_{\max} = \frac{2m_{eq} M \dot{r}_0 \beta_1^2 g_{31} L_p E_p (z - z_n)}{\sqrt{4K_{eq} m_{eq} M (m_{eq} + M) - C_{eq}^2 (m_{eq} + M)^{3/2}}} \exp\left(\frac{-\pi C_{eq} \sqrt{m_{eq} + M}}{\sqrt{4K_{eq} m_{eq} M - C_{eq}^2 (m_{eq} + M)^{1/2}}}\right) \times \left\{ \frac{\sin(\beta_1 x) + \sinh(\beta_1 x) + \kappa_1 (\cos(\beta_1 x) + \cosh(\beta_1 x))}{\phi_1(L)} \right\} \quad (28)$$

The output power of the piezoelectric device at location  $x$  from the clamped end of the beam is equal to  $P(x) = V^2(x)/R$ .

### Nominal case

The material and geometrical characteristics of the cantilever beam, piezoelectric patch, and the impact damper system are listed in Table 1. This system is subjected to initial displacements  $p_0 = q_0 = 10$  mm and the load resistance is equal to  $R_L = 52$  k $\Omega$ . Note that, according to the values, which are presented in Table 1, the

**Table 1.** Characteristics of the beam, piezoelectric patch, and impact damper system.

Properties of the cantilever beam	$E_b$ (GPa)	$L$ (mm)	$t_b$ (mm)	$W_b$ (mm)	$\rho_b$ (kg/m <sup>3</sup> )	$x_l$ (mm)
	200	80	5	5	7850	10
Piezoelectric PZT-5H (Priya and Inman, 2008)	$E_p$ (GPa)	$L_p$ (mm)	$t_p$ (mm)	$W_p$ (mm)	$\rho_p$ (kg/m <sup>3</sup> )	$g_{31}$ (V m/N)
	62	10	3	4	7800	0.008
Properties of the piezo-impact damper	$d$ (mm)	$m$ (kg)	$C_{eq}$ (N s/m)	$M$ (kg)	$K$ (N/m)	$C$ (N s/m)
	8	0.1	10	1	1000	0.1

PZT: lead zirconate titanate.

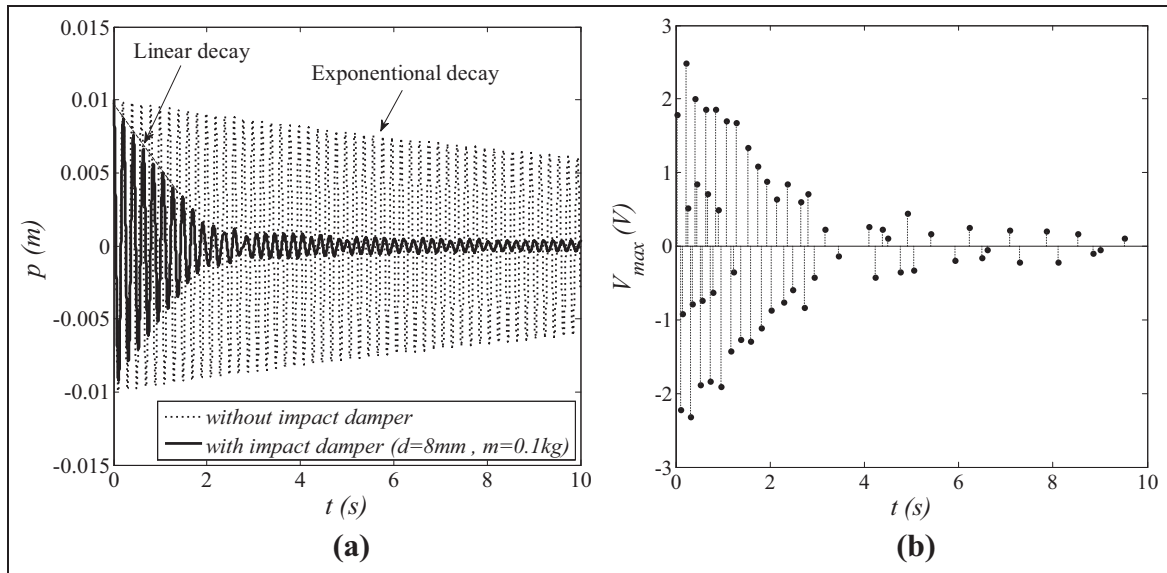


**Figure 3.** (a) Vibration of the main mass with and without impact damper and (b) output voltage of the piezoelectric beams.

equivalent mass and stiffness of the cantilever beam are equal to  $M_{eq} = 0.0292$  kg and  $K_{eq} = 46.7753$  MN/m.

### Results and discussion

As shown in Figure 3(a), the impact damper can strongly suppress vibrations of the main mass. The initially linear decrease in the maximum displacement of the main vibratory system, with the impact dampers, is usually represented by damping inclination, which is defined as

$$DI = \frac{(P_1 - P_2)}{(t_2 - t_1)} \tag{29}$$

where  $t_1$  and  $t_2$  are the times of occurrence of the maximum positive displacements  $P_1$  and  $P_2$ . The damping inclination can be considered as a parameter to measure the ability of impact dampers for suppressing undesired vibrations. Positive slope of the linear decay, which is shown in Figure 3(a), is equal to the damping inclination. The voltage delivered by each piezoelectric beam is shown in Figure 3(b). As shown in this figure, decreasing the amplitude of the main mass vibrations leads to decrease in the output voltage.

Discrete-time, cumulative root mean square (RMS) of the generated voltage values gives a measure of the average voltage, which is generated by each of the piezoelectric beams in the piezo-impact damper. This value, which is simply named as RMS output voltage, can be calculated using the following relation

$$V_{rms} = \left( \frac{1}{N} \sum_{i=1}^N \|V_i\|^2 \right)^{1/2} \tag{30}$$

where  $V_i$  is the output voltage from the piezoelectric device in the  $i$ th impact between the main mass and the impact mass. The main goals of designing a piezo-impact damper are twofold: (1) to increase the damping inclination and (2) maximizing the RMS output voltage. In doing so, in this study, the initial design of the piezo-impact dampers is divided into two parts. One of them is designing the impact damper, which can effectively suppress the vibratory response. For convenience, this type of design is named as “vibratory-based” design. The major consideration in the other kind of design, or simply “energy-based” design, is to have a system, which provides high values of output voltage.

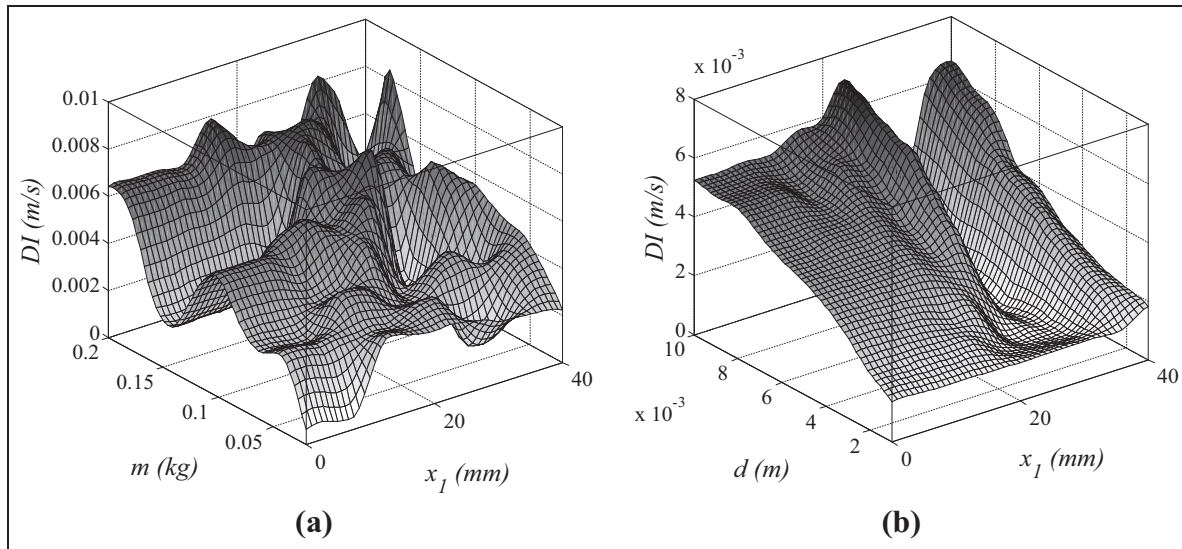


**Figure 4.** Variation in the damping inclination: (a) with  $x_1$  and  $m$  and (b) with  $x_1$  and  $d$ .

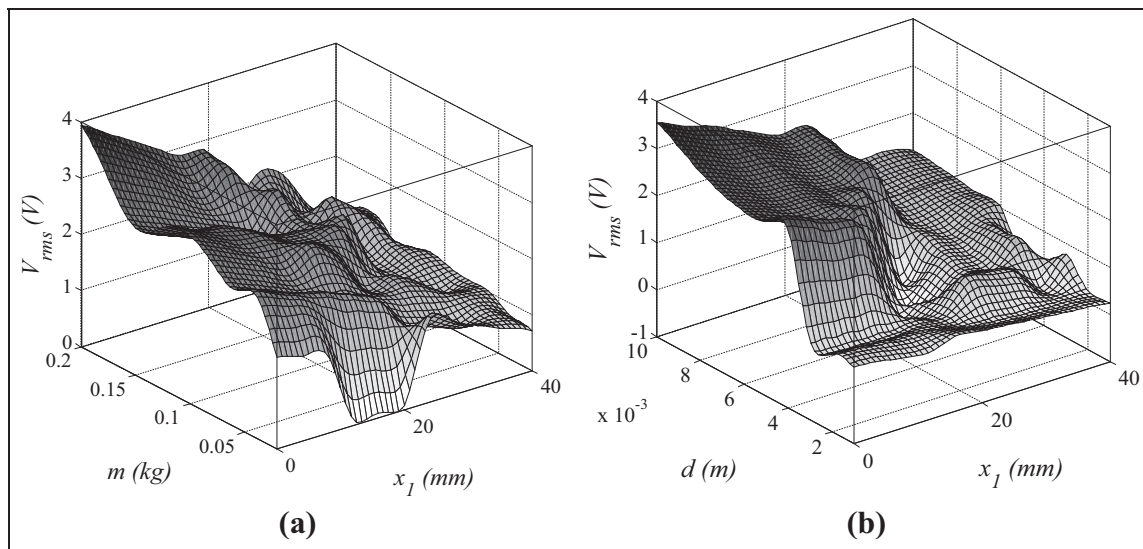


**Figure 5.** Variation in the RMS voltage: (a) with  $x_1$  and  $m$  and (b) with  $x_1$  and  $d$ . RMS: root mean square.

Combining the vibratory-based and the energy-based designs leads to make a perfect impact damper system. Note that the damping inclination should be mentioned when the vibratory-based design is considered. Variation in the damping inclination versus  $m$ ,  $x_1$ , and  $d$  is shown in Figure 4. As shown in this figure, the damping inclination randomly changes with  $m$  and  $x_1$ . Furthermore, it can be concluded that decreasing the gap size relatively decreases the damping inclination.

Based on energy consideration, the discussed piezo-impact damper is acceptably designed if the RMS output voltage was a high value. As shown in Figure 5, the output voltage does not uniformly vary with  $d$ ,  $m$ , and  $x_1$ . As shown in this figure, decreasing  $x_1$  and  $m$  leads

to a decrease in the damping inclination. Furthermore, increasing the distance of piezoelectric patch from the cantilevered end of beam ( $x_1$ ) leads to a decrease in the damping inclination.

Using the RMS output voltage, the average power delivered by the piezoelectric device can be calculated ( $P_{ave}(x) = V_{rms}^2/R$ ). Variation in the average power versus  $m$ ,  $x_1$ , and  $d$  is shown in Figure 6. As shown in this figure, like the RMS output voltage, the average power does not uniformly vary with  $d$ ,  $m$ , and  $x_1$ . Regarding Figures 5 and 6, it can be concluded that the behavior of the output power is similar to the RMS output voltage. Therefore, the ability of the energy harvesting can be presented using the RMS output voltage.



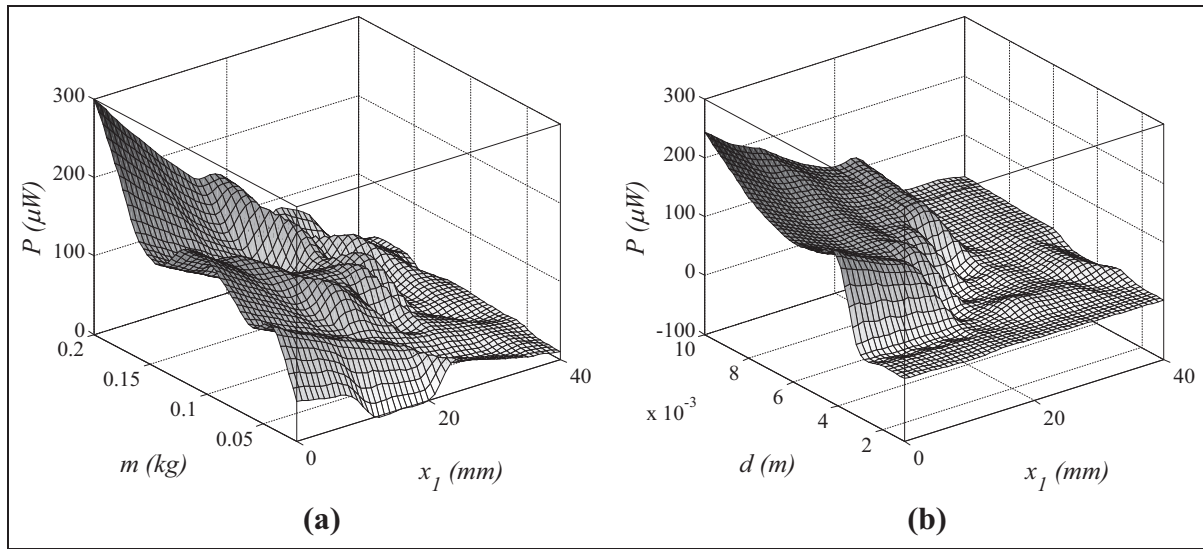


Figure 6. Variation in the average output power: (a) with  $x_1$  and  $m$  and (b) with  $x_1$  and  $d$ .

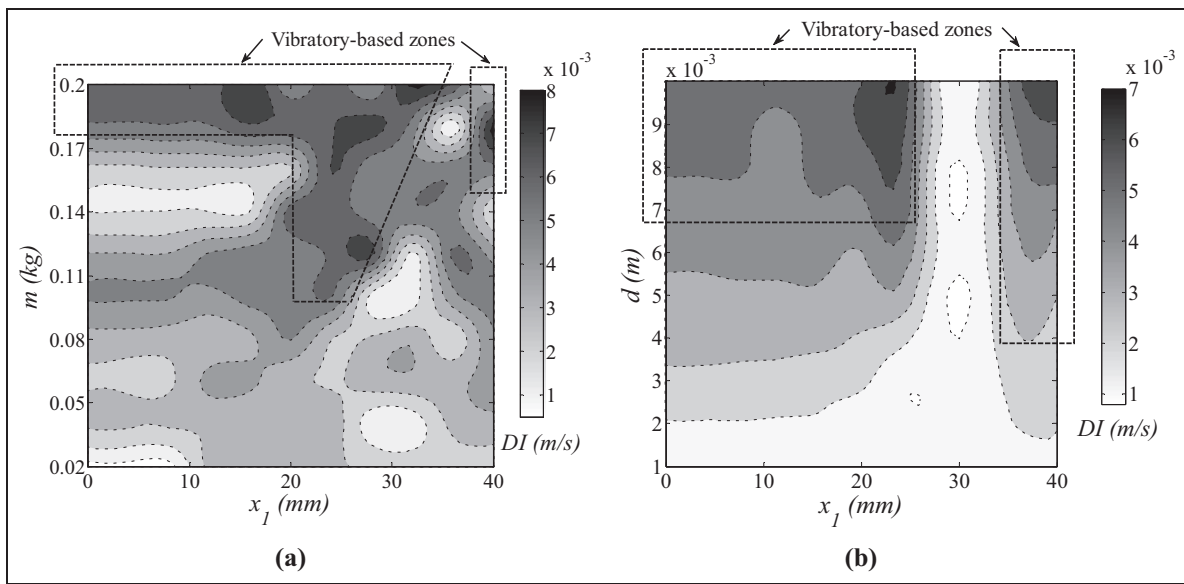


Figure 7. Variation in the damping inclination with (a)  $x_1$  and  $m$  and (b)  $x_1$  and  $d$ ; and the vibratory-based zones.

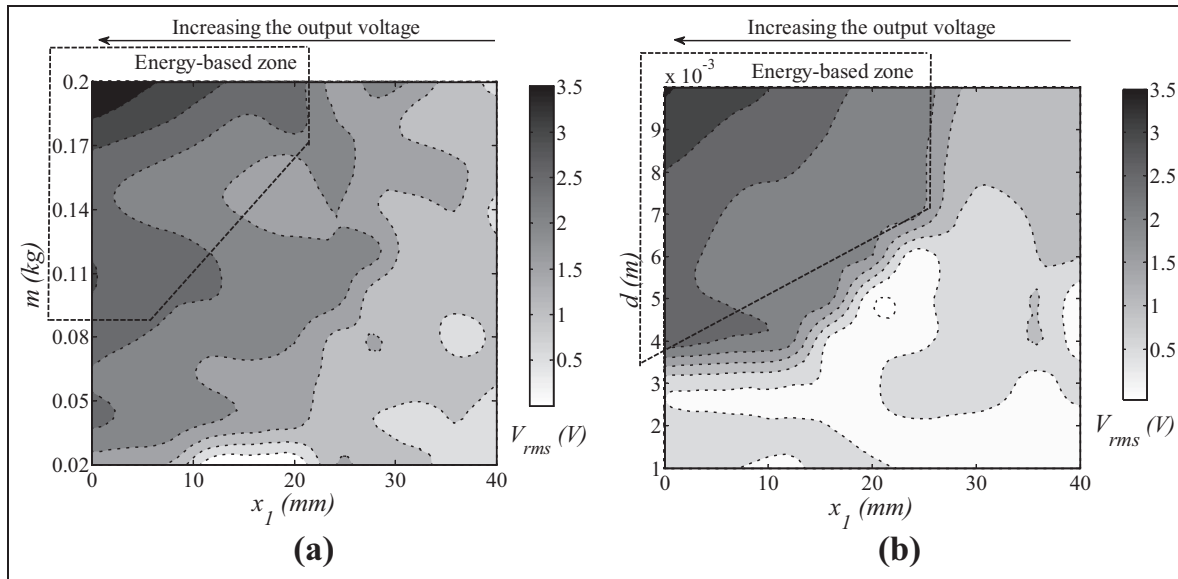
Variation in the damping inclination versus  $m$ ,  $d$ , and  $x_1$  is illustrated in Figure 7. As shown in this figure, because of random variation in the damping inclination, vibratory behavior of the piezo-impact damper cannot be predicted. To help the designer to select proper design parameter to have strong piezo-impact dampers, several design zones are introduced in Figure 7. Selecting the design parameters of the piezo-impact damper from these zones leads to have an impact damper, which can rapidly suppress undesired vibrations.

Figure 8 shows the variation in the RMS output voltage versus  $m$ ,  $d$ , and  $x_1$ . In this figure, the energy-based zones show appropriate ranges for selecting  $x_1$ ,  $d$ , and  $m$  to generate high values of energy.

To complete the initial design of the piezo-impact dampers, both vibratory-based and energy-based considerations should be considered. In doing so, the discussed design methods are summarized in a parameter named “perfectibility.” The so-called perfectibility is defined as follows

$$\text{Perfectibility} = \left( \frac{V_{rms}}{V_{rms, \max}} \times WF_1 + \frac{DI}{DI_{\max}} \times WF_2 \right) \times 100 \tag{31}$$

where  $WFs$  are the weight factors of each design. In this study, the weight factors are taken to be  $WF_1 = WF_2 = 0.5$ . If the perfectibility is high, it means that the



**Figure 8.** Variation in the RMS output voltage (a) with  $x_1$ ,  $m$  and (b)  $x_1$ ,  $d$ ; and the energy-based zones. RMS: root mean square.

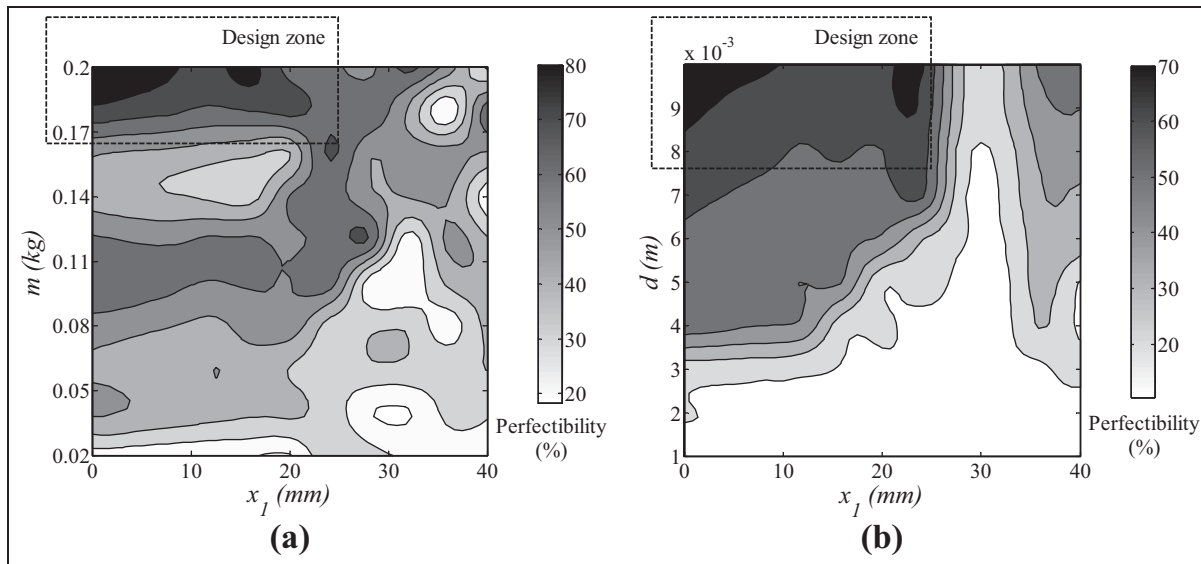


**Figure 9.** Design zones with respect to (a)  $m$  and  $x_1$  and (b)  $d$  and  $x_1$ .

piezo-impact damper will be a good energy harvester and vibration suppressor. Variation in the perfectibility versus  $m$ ,  $d$ , and  $x_1$  is shown in Figure 9. As shown in this figure, to have a well-designed piezo-impact damper, parameter  $m$  should be selected between 0.17 and 0.20 kg, parameter  $d$  should be selected between 8 and 10 mm, and parameter  $x_1$  should be selected between 0 and 25 mm.

The effect of selecting parameters of the piezo-impact damper from the vibratory-based zone and the energy-based zone is clearly shown in Figure 10. In this figure, vibration of the main mass and RMS output

voltage for two piezo-impact dampers are presented. One of the piezo-impact dampers, unlike the other, is designed regarding the vibratory-based and the energy-based considerations.

As shown in Figure 10, the piezo-impact damper, which is designed based on vibratory and energy considerations, works strongly better than the other impact damper. In other words, the piezo-impact damper, the parameters of which are selected from the design zones ( $x_1 = 0.01$  m,  $m = 0.2$  kg, and  $d = 0.01$  m), can suppress vibration better than the other piezo-impact damper, the parameters of which are not located in the

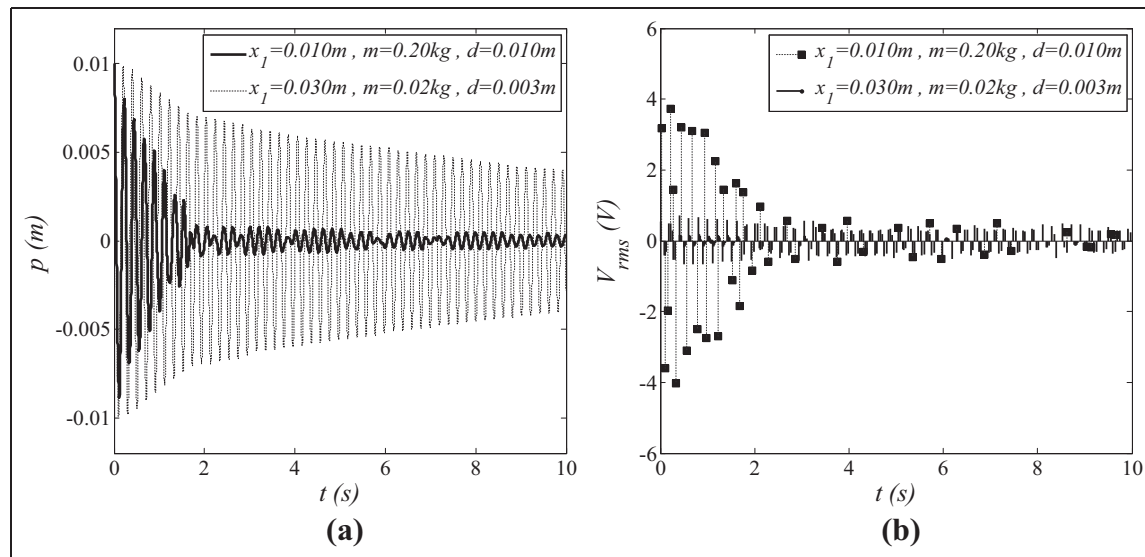


**Figure 10.** Comparison between (a) vibratory-based and (b) energy-based behavior of a perfectly designed piezo-impact damper ( $x_1 = 1$  cm,  $d = 1$  cm) and another vibro-impact system ( $x_1 = 3$  cm,  $d = 3$  mm).

design zones ( $x_1 = 0.03$  m,  $m = 0.02$  kg, and  $d = 0.003$  m). Furthermore, the perfectly designed piezo-impact damper can harvest energy more than the other impact damper. For the perfectly designed piezo-impact damper,  $DI = 0.6325$  cm/s and  $V_{rms} = 3.6094$  V. In the other piezo-impact damper, which is not designed regarding the vibratory and energy considerations,  $DI = 0.1236$  cm/s and  $V_{rms} = 0.4032$  V.

## Conclusion

In this study, the application of the piezo-impact dampers is investigated. The barriers of the piezo-impact dampers are equipped with the piezoelectric patches. It is shown that such system suppresses undesired vibration of the main vibratory mass and then converts it into a useful energy. Dependence of the output voltage to the barrier deformation is theoretically studied. It is shown that the output voltage directly varies with the maximum deformation of the cantilever beams, which are used as the barriers.

Variation in the damping inclination and the output voltage generated by the piezo-impact damper is studied with varying the gap size, mass ratio, and location of the piezoelectric patch on the barrier. The vibratory-based and energy-based designs are introduced regarding the ability of vibration suppressing and energy harvesting, respectively. Based on the discussed design methods, six suitable design zones are defined. It is shown that using the so-called perfectibility, the six suitable zones can be summarized in only two zones.

To provide a perfectly designed piezo-impact damper, based on the discussed design methods, two user-oriented charts are presented. The effect of selecting the

design parameters of the piezo-impact damper from the suitable design zones is studied on the application of the system. As a result, it is shown that considering suitable design parameters can, respectively, increase the RMS output voltage and the damping inclination more than 795% and 411%.

## Declaration of conflicting interest

The authors declared no potential conflicts of interest with respect to the research, authorship, and/or publication of this article.

## Funding

This research received no specific grant from any funding agency in the public, commercial, or not-for-profit sectors.

## References

- Abdelkefi A, Barsallo N, Tang L, et al. (2013a) Modeling, validation, and performance of low-frequency piezoelectric energy harvesters. *Journal of Intelligent Material Systems and Structures*. DOI: 10.1177/1045389X13507638.
- Abdelkefi A, Hajj MR and Nayfeh AH (2013b) Piezoelectric energy harvesting from transverse galloping of bluff bodies. *Smart Materials and Structures* 22: 015014.
- Abdelkefi A, Yan Z and Hajj MR (2013c) Modeling and non-linear analysis of piezoelectric energy harvesting from transverse galloping. *Smart Materials and Structures* 22: 025016.
- Abdelkefi A, Yan Z and Hajj MR (2014) Performance analysis of galloping-based piezoaeroelastic energy harvesters with different cross-section geometries. *Journal of Intelligent Material Systems and Structures* 25: 246–256.
- Afsharfard A and Farshidianfar A (2012a) Design of non-linear impact dampers based on acoustic and damping

- behavior. *International Journal of Mechanical Sciences* 65: 125–133.
- Afsharfard A and Farshidianfar A (2012b) An efficient method to solve the strongly coupled nonlinear differential equations of impact dampers. *Archive of Applied Mechanics* 82: 977–984.
- Agneni A and Coppotelli G (2004) Modal parameter prediction for structures with resistive loaded piezoelectric devices. *Experimental Mechanics* 44: 97–100.
- Agneni A, Mastroddi F and Polli GM (2003) Shunted piezoelectric patches in elastic and aeroelastic vibrations. *Computers & Structures* 81: 91–105.
- Annandas VG and Radhika MA (2013) Electromechanical impedance of piezoelectric transducers for monitoring metallic and non-metallic structures: a review of wired, wireless and energy-harvesting methods. *Journal of Intelligent Material Systems and Structures* 24: 1021–1042.
- Bapat CN and Sankar S (1985) Single unit impact damper in free and forced vibration. *Journal of Sound and Vibration* 99: 85–94.
- Ba'zant ZP and Cedolin L (2010) *Stability of Structures: Elastic, Inelastic, Fracture and Damage Theories*. Hackensack, NJ/London: World Scientific Publishing.
- Cheng CC and Wang JY (2003) Free vibration analysis of a resilient impact damper. *International Journal of Mechanical Sciences* 45: 589–604.
- Cheng J and Xu H (2006) Inner mass impact damper for attenuating structure vibration. *International Journal of Solids and Structures* 43: 5355–5369.
- Dadfarnia M, Jalili N, Xian B, et al. (2004) A Lyapunov-based piezoelectric controller for flexible Cartesian robot manipulators. *Journal of Dynamic Systems, Measurement, and Control: Transactions of the ASME* 126: 347–358.
- De Jong PH, de Boer A, Loendersloot R, et al. (2013) Power harvesting in a helicopter rotor using a piezo stack in the lag damper. *Journal of Intelligent Material Systems and Structures* 24: 1392–1404.
- De Marqui C and Erturk A (2013) Electroaeroelastic analysis of airfoil-based wind energy harvesting using piezoelectric transduction and electromagnetic induction. *Journal of Intelligent Material Systems and Structures* 24: 846–854.
- Dimentberg MF and Iourtchenko DV (2004) Random vibrations with impacts: a review. *Nonlinear Dynamics* 36: 229–254.
- Ema S and Marui E (1994) A fundamental study on impact dampers. *International Journal of Machine Tools & Manufacturing* 34: 407–421.
- Erturk A and Inman DJ (2008) A distributed parameter electromechanical model for cantilevered piezoelectric energy harvesters. *Journal of Vibration and Acoustics* 130: 041002.
- Erturk A, Vieira WGR, De Marqui C, et al. (2010) On the energy harvesting potential of piezoaeroelastic systems. *Applied Physics Letters* 96: 184103.
- Green PL, Papatheou E and Sims ND (2013) Energy harvesting from human motion and bridge vibrations: an evaluation of current nonlinear energy harvesting solutions. *Journal of Intelligent Material Systems and Structures* 24: 1494–1505.
- Ibrahim RA (2009) *Vibro-Impact Dynamics: Modeling, Mapping and Applications*. Berlin: Springer-Verlag.
- Jacquelin E, Adhikari S and Friswell MI (2011) A piezoelectric device for impact energy harvesting. *Smart Materials and Structures* 20: 105008.
- Kim I-H, Jang S-J and Jung H-J (2013) Performance enhancement of a rotational energy harvester utilizing wind-induced vibration of an inclined stay cable. *Smart Materials and Structures* 22: 075004.
- Mehmood A, Abdelkefi A, Hajj MR, et al. (2013) Piezoelectric energy harvesting from vortex-induced vibrations of circular cylinder. *Journal of Sound and Vibration* 332: 4656–4667.
- Moss SD, McLeod JE and Galea SC (2013) Wideband vibro-impacting vibration energy harvesting using magnetoelectric transduction. *Journal of Intelligent Material Systems and Structures* 24: 1313–1323.
- Palm WJ (2007) *Mechanical Vibration*. Hoboken, NJ: John Wiley & Sons.
- Poppowell N and Liao M (1991) A simple design procedure for optimum impact dampers. *Journal of Sound and Vibration* 146: 519–526.
- Pozzi M and Zhu M (2012) Characterization of a rotary piezoelectric energy harvester based on plucking excitation for knee-joint wearable applications. *Smart Materials and Structures* 21: 055004.
- Priya S and Inman DJ (2008) *Energy Harvesting Technologies*. New York: Springer.
- Sadd MH (2009) *Elasticity: Theory, Applications, and Numerics*. Amsterdam/Boston, MA: Elsevier/AP.
- Simites GJ and Hodges DH (2006) *Fundamentals of Structural Stability*. Amsterdam/Boston, MA: Elsevier/Butterworth-Heinemann.
- Son L, Hara S, Yamada K, et al. (2010) Experiment of shock vibration control using active momentum exchange impact damper. *Journal of Vibration and Control* 16: 49–64.
- Soong TT and Spencer BF Jr (2002) Supplemental energy dissipation: state-of-the-art and state-of-the-practice. *Engineering Structures* 24: 243–259.
- Tang L, Yang Y and Soh CK (2010) Toward broadband vibration-based energy harvesting. *Journal of Intelligent Material Systems and Structures* 21: 1867–1897.
- Thomson WT (1993) *Theory of Vibration with Applications*. Englewood Cliffs, NJ: Prentice Hall.
- Ugural AC and Fenster SK (2011) *Advanced Mechanics of Materials and Elasticity*. Upper Saddle River, NJ: Prentice Hall.
- Zhang D-G and Angeles J (2005) Impact dynamics of flexible-joint robots. *Computers & Structures* 83: 25–33.
- Zhao L, Tang L and Yang Y (2013) Comparison of modeling methods and parametric study for a piezoelectric wind energy harvester. *Smart Materials and Structures* 22: 125003.
- Zinjade PB and Mallik AK (2007) Impact damper for controlling friction-driven oscillations. *Journal of Sound and Vibration* 306: 238–251.